Computation of the RCS of Complex Bodies Modeled Using NURBS Surfaces

M. Domingo, F. Rivas, J. Pérez, R. P. Torres, M. F. Cátedra
Departamento de Electrónica
Universidad de Cantabria
39005 Santander
Spain
Tel: +34 42 201493
Fax: +34 42 201873
E-mail: felipe@gsr.unican.es

1. Abstract

This paper presents the *RANURS* code (RAdar cross section–NURbS surfaces) for the analysis of the monostatic radar cross section (RCS) of electrically large complex targets. The geometric representation of the targets is given in terms of parametric surfaces, which allow an excellent fit between the model and the real surface. The parametric surfaces used are NURBS (Non-Uniform Rational B-Spline) surfaces. This technique of modeling is currently used in many industries to represent complex bodies such as aircraft, ships, etc. Today, most of the CAGD (Computer Aided Geometric Design) tools use the NURBS format for modeling, because it can represent complicated objects using limited information. Therefore, an important feature of the code is its compatibility with most of the available CAGD codes, in order to ensure that the entire design process, involving different engineering aspects (structural, mechanical, aerodynamical, electrical, etc.) can be developed with compatible models.

The scattered fields are calculated by using the Physical Optics and the Equivalent Currents Methods (PO+ECM). The following contributions to the RCS are taken into account: Reflected field, diffracted field, double-reflected field, and diffracted-reflected field. In addition, a method for determining the hidden parts of the targets is used. The PO+ECM approach is directly applied on the parametric surfaces, and the final expressions of the fields are given as functions of the coefficients of the numerical description of the NURBS patches.

2. Introduction

The knowledge and reduction of the RCS of vehicles has been a requirement of the aerospace industry for the last 20 years. The RCS prediction codes offer a cheaper alternative to measuring a target at a RCS range. Moreover, the codes can be used in the initial steps of the design process, before the vehicles have been physically built. Because of the aforementioned reasons, RCS computation has been one of the main areas of intensive research work. In fact, the Spanish aeronautical industry, led by Construcciones Aeronauticas SA (CASA), launched a national consortium (1988), which united several research groups. The objective of the project was to provide the Spanish industry with the tools to predict and measure the radar cross section of complex bodies.

The code *RANURS* is one of the University of Cantabria's contributions to the consortium's activities in the area of high-frequency RCS prediction. It can be considered an evolution of a previous program called *TOTAL*. The code *TOTAL* works over an edge-facet model of the target, similar to the program *RECOTA* [1]. Furthermore, the *TOTAL* program includes a very efficient treatment of double reflections and diffraction-reflections [2, 3].

Although the edge-facet model, used in conjunction with the PO+EMC approach, gives good results and a big improvement over other geometrical descriptions [1, 2], it has a major disadvantage: a large number of facets is necessary in order to fit curved surfaces. As a general rule of thumb, the number of facets must be large enough to provide a maximum distance of $\lambda/16$ between the real curved surface and the flat facets. The solution chosen was to use NURBS surfaces [4-6], which provide an efficient and accurate description of curved surfaces (they include plane surfaces as a special case). The method developed in *RANURS* works directly with the NURBS surfaces' parameters, and provides expressions of the scattered field in terms of these parameters.

The use of the NURBS description of objects for RCS computation was introduced simultaneously by some Spanish research groups [7-11]. At present, the NURBS surfaces for the description of objects are being introduced in other electromagnetic applications [12-13]. In the case of RCS computation, a notable example is the code *GRECO* [10]. This code makes use of the NURBS technique for modeling the object geometry and, after using a graphical-processing approach, an image of the target on the computer screen is used to obtain the unit normal vector at each point (pixel) on the visible surface. With this information, a PO/PTD approximation of the RCS is obtained. The major advantage of the graphical-processing technique is that the shadowing is performed efficiently, but the drawback is that *GRECO*, in fact, works with a faceted model, pixel by pixel. As a result, interactions like double reflections and diffraction-reflections are quite difficult to include.

Another advanced and complete code, based on the direct application of PO to parametric curved surfaces, is *CADDSCAT* [14]. This code has been developed at McDonnell Douglas Aerospace. In *CADDSCAT*, physical optics are applied by combining numerical integration with an analytic technique on bi-cubic patches. Perhaps the more critical points are the increase of run times with frequency, and the cumbersome treatment of shadowing. On the other hand, this code offers such interesting capabilities as the ability to handle RAM (radar-absorbing-material)-treated surfaces, gap diffractions, sea-state modeling, etc.

At high frequencies, the different parts of a body are practically uncoupled; therefore, the *TOTAL* scattering field can be computed by adding contributions from local-scattering centers. As

long as this is true, a geometric model built from elements like patches, is very suitable, because the contributions to the scattered field from patches and edges are accurately calculated using the PO+ECM approach [1-3]. In fact, an efficient method for applying PO directly over NURBS patches has been developed [7-9]. The diffracted field is taken into account by applying the Equivalent Current Method over the edges. Double effects, between patches and edges, are incorporated for the cases of plane facets and straight edges by following the techniques developed in [2-3].

Therefore, in *RANURS*, the RCS of a body is calculated by adding the contributions of the following scattering mechanisms:

- Reflected field
- Diffracted field
- Double-reflected field
- Diffracted-reflected field

Shadowing is also given careful consideration, because of its important contribution to the accuracy and efficiency of the method.

This paper does not present a detailed description of the theories, approaches, and techniques involved in the *RANURS* code; rather, it presents an overview of the subject. Companion papers and references, which can be consulted for more detailed explanations, are [2-3] and [7-9]. The rest of the paper is ordered as follows. Section 3 presents some ideas about target modeling, and the features of using NURBS surfaces. In Section 4, the fundamentals of applying PO to NURBS surfaces are summarized. Section 5 is devoted to explaining the approach followed in order to account for diffracted fields. In Section 6, the double effects are considered. Issues about shadowing are discussed in Section 7. Section 8 highlights some results, which are followed by the major conclusions in Section 9.

3. Target modeling

Until now, the plane-facet representation has been the most extensively used method for the geometric description of RCS targets [1-2]. In this method, the bodies are described in terms of facets and wedges. This technique is referred to as the method of components using facets and wedges. Some of its principal advantages lie in its simplicity, and in its capacity to represent any geometry.

An alternative to the previous technique is the method of components using NURBS curves and surfaces [4-6]. These are free-form parametric curves and surfaces. Today, the NURBS format is in widespread use in the world of CAGD. It is currently used in the aeronautic, automobile, ship, and other industries, in both the designing and manufacturing stages. The NURBS scheme is able to manipulate both free-form surfaces and primitive quadrics (cylinders, spheres, cones, etc.). Linear surfaces (plane facets) are an additional, special case of NURBS surfaces. Using this technique, it is possible to model complicated bodies with a low number of patches, and, therefore, with limited information. For instance, a primitive quadric, like a cylinder, can be modeled exactly as a single NURBS surface. A complicated body, such as a complete aircraft, can be described with high precision by using less than one hundred NURBS surfaces (see Figure 1).

NURBS curves and surfaces have been an Initial Graphics Exchange Specification (IGES) standard since 1983 [15]. IGES is the standard for the interchange of design information between various computer-aided-design systems, and between computer-aided design and computer-aided manufacturing systems. This standard has been in operation for approximately 15 years, and is widely accepted by aircraft companies, as well as by the US government. NURBS has been incorporated into a number of geometric-modeling systems. It has also been implemented in hardware (VLSI or microcode) by a number of graphics-workstation manufacturers. Today, many of the available CAGD tools provide descriptions of the designed objects in terms of NURBS curves and
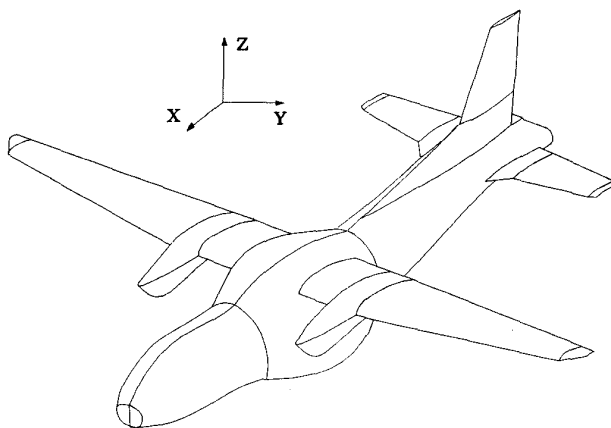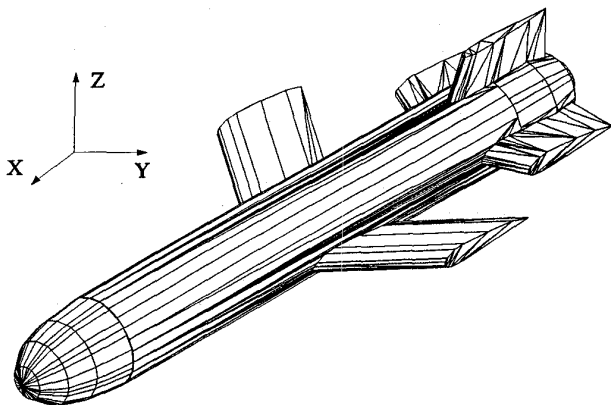

Figure 1. A NURBS-patch model of the CN-235 aircraft.

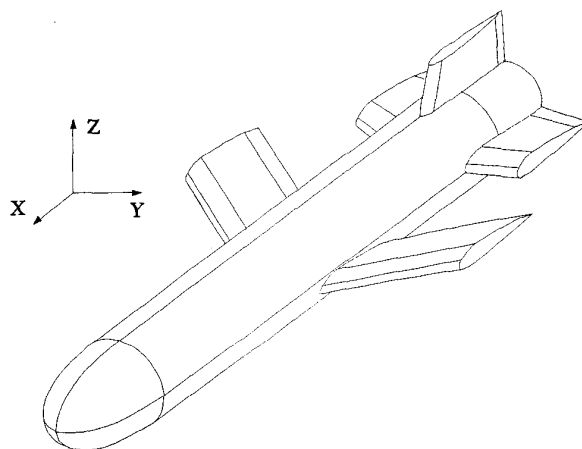Figure 2a. A plane-facet model of a generic missile.

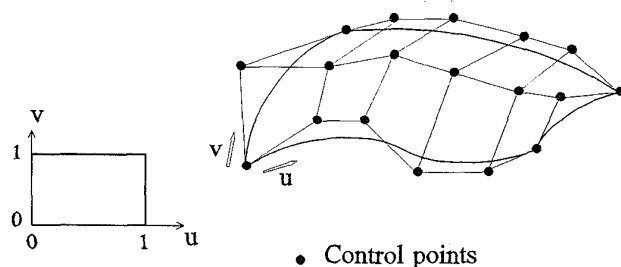Figure 2b. A NURBS surface model of a generic missile.

Figure 3. A NURBS surface-geometric description.

surfaces. One of them is the *I-DEAS* solid-modeling tool [16]. It is integrated with *RANURS* as pre-processing software, achieving the following tasks:

- Target modeling
- Target visualization
- NURBS surface generation

However, many other CAGD tools can be easily integrated with *RANURS* via IGES format.

Apart from the above features, the use of NURBS patches provides other important advantages in the description of bodies for RCS computation, with regard to the plane-facet approximation:

- It includes the plane facets as a special case of NURBS surfaces.

- The number of surfaces required to describe complex bodies is very low. Figures 2a and 2b show a representation of a generic missile, using flat facets and NURBS surfaces, respectively.

- A better fit to the target geometry is achieved. Thus, "facet noise," usually present in the "facet-modeling" codes, is avoided. In fact, in many cases the model is completely identical to the real body, because the NURBS scheme is used in the design and manufacturing process of the object.

- Artificial edges are not introduced.

A NURBS patch is a parametric surface of arbitrary degree (see Figure 3) [4-6]. It is defined by a set of control points with associated weights, and two knot vectors (one for each parametric coordinate). The parametric coordinates vary between 0 and 1, so the surface domain is a square of side 1. The description of each edge as a NURBS curve is obtained directly from the geometric information of the NURBS surfaces which form the edge.

Any NURBS representation can also be written in terms of piecewise-Bezier patches [4-5]. A Bezier patch is also a parametric surface, defined as a linear combination of a set of control points and the Bernstein polynomials [4]. Bezier patches are more suitable for the numerical computation of parameters associated with the surface (derivatives, normal vectors, curvatures, etc.), due to the characteristics of the Bernstein basis. On the other hand, a mesh of NURBS elements is the best tool for constructing and storing the surface of complex objects. It is relatively simple and fast to obtain the Bezier mesh from a NURBS representation, by applying the Cox-De Boor algorithm [17]. Most of the available CAGD software uses NURBS surfaces for the design and storage of the body shape, and the Bezier format for the numerical computations (rendering) with the surface.

The number of Bezier patches obtained from a NURBS representation, and the information about the order of continuity between adjacent patches, depends on their knot vectors. A rational-Bezier patch is also defined by two degrees (one for each parametric coordinate), a mesh of control points, and a set of associated weights. The number of points of the mesh depends on the degrees. The parametric domain is a square of corners $(0,0)$, $(0,1)$, $(1,0)$, $(1,1)$. The surface points of a rational-Bezier surface are given by

$$\vec{r}(u,v) = \frac{\sum_{i=0}^{m}\sum_{j=0}^{n} w_{ij}\vec{b}_{ij}B_i^m(u)B_j^n(v)}{\sum_{i=0}^{m}\sum_{j=0}^{n} w_{ij}B_i^m(u)B_j^n(v)}, \qquad (1)$$

where the $\vec{b}_{ij}$ are the control points, the w_{ij} are the control-point weights, m and n are the surface degrees, and B_i^m and B_j^n are the Bernstein polynomials. Also, the parametric derivatives of the surface can be written as a function of the patch degrees, control points, weights, and Bernstein bases [4].

The Bezier surfaces can be easily classified into four types, depending on geometric criteria (see Figure 4), using information about the degrees and the mesh of control points [8-9]:

a. Polygonal-plane facets:

A Bezier surface is flat if the mesh of control points is located in a plane, and polygonal if the boundary-control points of each side of the mesh are collinear (see Figure 4a). In this case, the vertices of the polygon coincide with the control points of the corners of the mesh.

b. Plane patches with curved boundaries:

All the control points are in the same plane, but on at least on one boundary, they are not collinear (see Figure 4b). This implies that at least one of the surface degrees must be greater than one. A typical example is a disk.
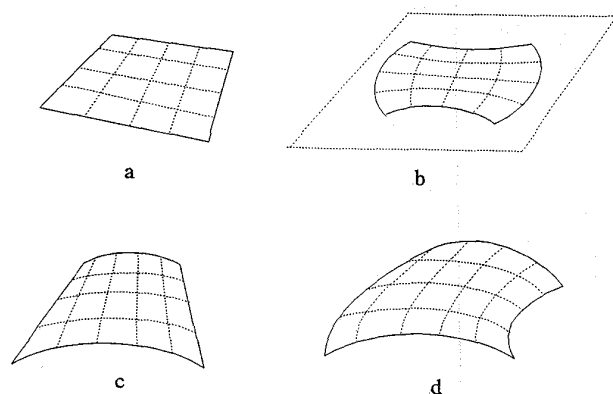

Figure 4. Classification of the Bezier surfaces: a. Polygonal plates; b. Plane patches with curved boundaries; c. Singly curved surfaces; and d. Doubly curved surfaces.

c. Singly curved surfaces:

These are the so-called ruled surfaces (see Figure 4c). They are curved surfaces generated by a family of straight lines. These lines are isoparametric segments, so the patch equations are linear for one of the parametric coordinates [4]. Typical examples are cylindrical and conical surfaces. Ruled-Bezier surfaces may be easily identified from their geometric descriptions [11].

d. Doubly curved surfaces:

This group comprises all patches not included under the previous categories, whose surface equations are not linear for either of the two parametric coordinates (see Figure 4d).

4. Reflected field

As described in the introduction, the reflected field is calculated by using the PO approximation. Given an incident monochromatic plane wave, under the far-field approximation, the backscattered field of an arbitrary conducting body, predicted by the PO theory [18-20], is given by

$$\vec{E}_s(\mathbf{r}) = -j\lambda^{-1}\vec{E}_0 \frac{e^{-jKr}}{r}I, \qquad (2)$$

$$I = \int_S \left[\hat{K} \cdot \hat{n}_s(\vec{r}')\right]e^{2j\vec{K}\cdot\vec{r}'}ds', \qquad (3)$$

where S is the illuminated surface of the body, λ is the wavelength, $\vec{E}_0$ is the incident electric field, $\vec{K}$ is the wave vector, $\hat{K}$ is the normalized wave vector, $\vec{r}'$ is the surface point corresponding to ds', and $\hat{n}_s$ is the unit-normal vector at this point. I is the so-called PO integral. First, notice that the incident field and the predicted PO-scattered field have the same polarization. Second, notice that the monostatic-RCS prediction, due to this mechanism, is independent of the incident-wave polarization.

The main difficulty in evaluating the scattered field is the computation of the PO integral. This is evaluated as the sum of the contributions of all the Bezier patches of the model. The method of calculation of the integral differs, depending on the patch geometry.

a. Polygonal plane facets

If the surface is plane, $\hat{n}_s(\vec{r}')$ is constant, so Equation (3) can be calculated using Gordon's method [21]. In this case, the PO integral is reduced to a closed-form expression, involving no integrations at all.

b. Plane patches with curved boundaries

Approximate boundaries can be drawn with polylines, obtained directly from the control points of the surface, and then Equation (3) can be calculated in the same way as for the polygons.

c. and d. Singly and doubly curved surfaces

Most of the surfaces of a real target are curved, but in this case, it is usually impossible to evaluate the PO integral analytically. Therefore, it is necessary to use approximate methods in order to evaluate the field scattered from curved patches.

For parametric surfaces, the PO integral, Equation (3), can be expressed as a function of the parametric coordinates. This is done

by writing the normal vector and the surface element in terms of the parametric derivatives of $\vec{r}(u,v)$, i.e., $\vec{r}_u, \vec{r}_v$ respectively [8]:

$$\vec{I} = \int_{u=0}^{u=1}\int_{v=0}^{v=1}\vec{r}_u(u,v) \times \vec{r}_v(u,v)e^{2j\vec{K}\cdot\vec{r}(u,v)}dudv. \qquad (4)$$

The integration domain is the surface-parametric domain, which is a square of side 1. The integral is evaluated using the stationary-phase method (SPM) [22]. It provides an asymptotic expansion of the PO integral, valid for small values of the wavelength with respect to the surface dimensions. Reference [8] presents the mathematical expressions of the asymptotic expansion, and the geometrical meaning of the leading terms.

In doubly curved patches, the SPM contributions are only derived from regions around certain critical points of the integral domain. Furthermore, different types of critical points give rise to different powers of K in the leading terms of their respective contributions. There are three types of critical points: stationary-phase points, boundary-critical points, and vertex points (see Figures 5, 6, and 7).

In singly curved surfaces, the phase term of the integral, Equation (4), is linear for one parametric coordinate. In this case, the integration along this coordinate can be calculated analytically, and the SPM for single integrals is applied to evaluate the integral along the other coordinate. Consequently, larger contributions are produced by regions surrounding certain critical isoparametric seg-
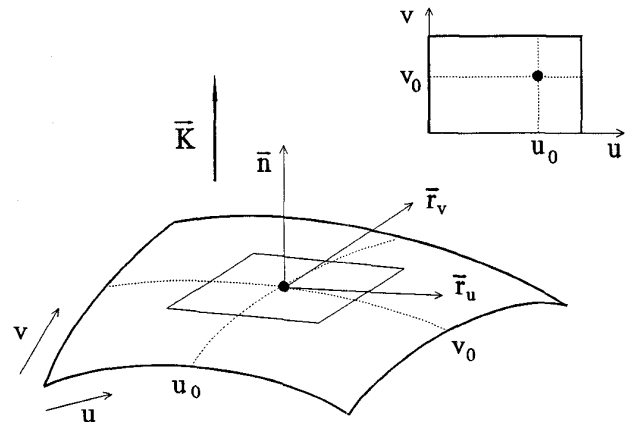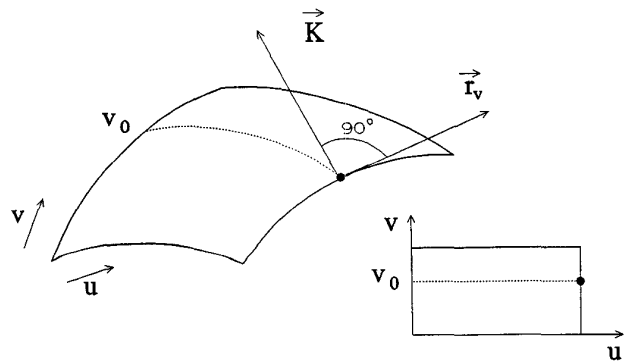

Figure 5. A stationary-phase point.
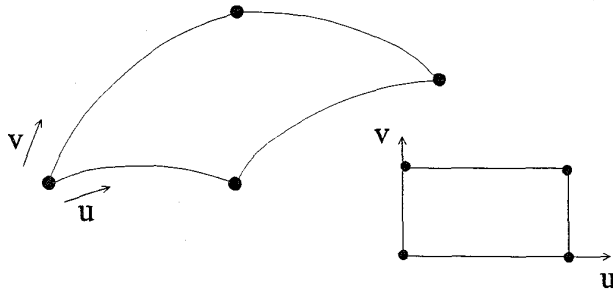

Figure 6. A boundary critical point.
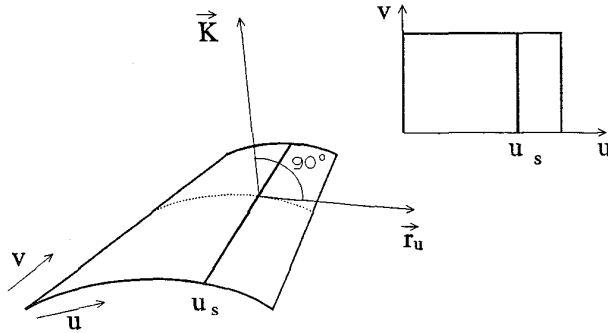
Figure 7. Vertex points.
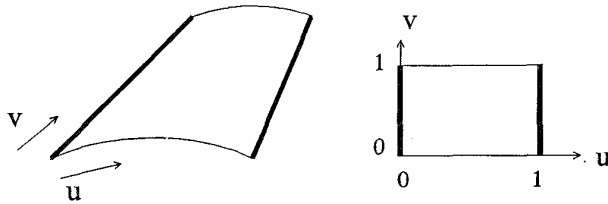

Figure 8. Stationary-phase segments.

Figure 9. Boundary segments.

ments on the surface, and different types of critical segments in turn give rise to different powers of K. These are the so-called stationary and boundary segments (see Figures 8 and 9).

5. Diffracted field

The PO predictions can be improved, when non-uniform currents due to the edges are added to the uniform current induced in the surface. The reason is that the current generated in the surface is different from the PO current, in the proximity of the patch boundaries.

The PO-ECM approximation is an efficient technique for calculating the RCS from targets modeled in terms of plane-polygonal patches and straight edges [1-3]. This approach has been used in several codes using edge-facet models, in which the artificial edges, i.e., those generated as result of the faceting of the model, must also be considered. Using *RANURS*, no artificial edges are introduced when model faceting is implemented, and, therefore, only the body's inherent edges should be considered. This means that *RANURS* is more accurate and efficient than codes which introduce artificial edges.

The calculation of the diffracted field by edges is carried out in an analytic form, by the equivalent-current method. In order to form these currents, a set of PTD coefficients [18, 23] is used, so that the diffracted field is compatible with the PO results. Because the analysis is restricted to the backscattering directions, the Knott and Senior equivalent currents [18, 23] have been selected, since they are simple to apply, and provide correct solutions in the Keller cone.

The non-uniform equivalent currents on the edges are formulated as follows:

$$I_e(\vec{r}_s) = \frac{2\,ji(\hat{t}\cdot\vec{E}^i)}{K_0 Z_0 \sin\beta^i \sin\beta^s}\, f(\delta^i,\delta^s), \qquad (5)$$

$$I_m(\vec{r}_s') = \frac{2\,ji(\hat{t}\cdot\vec{H}^i)}{K_0 Z_0 \sin\beta^i \sin\beta^s}\, g(\delta^i,\delta^s), \qquad (6)$$

where $\hat{t}$ is the unit vector tangent to the edge; $\vec{E}^i$ and $\vec{H}^i$ are the incident electric and magnetic incident fields; Z_0 and Y_0 are the impedance and admittance of free space, respectively; β^i and β^s are the angles between the edge, and the incident and diffracted directions, respectively; f and g are the Ufimtsev diffraction coefficients, when the scattering direction is close to the Keller cone; and δ^i and δ^s are the angles between the incident and the scattering directions and the top surface of the wedges, respectively. These are measured in the plane normal to the wedge length.

6. Double effects

Although at high frequencies, most parts of a scatterer are uncoupled, there are some geometric configurations and incident directions where the interactions between different parts become relevant. The most relevant interactions can be reduced to

1. Double reflections by facets
2. Diffraction by an edge and reflection by a plane facet
3. Reflection by a plane facet and diffraction by an edge

6.1 Double-reflected field

Double reflections between facets have been studied by many authors [25-28]. The classical methods used for the analysis of double interactions between patches have applied the Physical Optics-Physical Optics (PO-PO) and Geometric Optics-Physical Optics (GO-PO) approaches.

The PO-PO approach is very cumbersome and time-consuming, because it requires the computation of a pair of nested double integrals. The problem is simplified if the first reflection is evaluated by using GO, as is involved in the GO-PO approach. Applying GO-PO, the plane nature of the wave is maintained from the first reflection, and the radiated field from the second illuminated surface can be obtained analytically (PO integral). The GO-PO approach loses validity when a dihedral structure is formed by electrically small patches, or when the internal angle is too acute. Fortunately, these geometric configurations are not frequently found in usual targets.

The *RANURS* code takes into account the contributions between polygonal patches that form dihedral corners close to 90° by using GO-PO. However, unlike other studies [25, 27], where the

solution is limited to the analysis in the plane perpendicular to the axis of the dihedral, in *RANURS* the problem has been generalized to include arbitrary spatial position, arbitrary geometries, and general observation angles. The GO contribution to this approach consists of applying the image theory through a conducting finite facet. A sketch of the problem is shown in Figure 10. The source currents could be expressed as

$$\vec{J}(\vec{r_s'}) = \left(J_x\hat{x} + J_y\hat{y} + J_z\hat{z}\right)e^{-j\vec{K}^i\cdot\vec{r_s'}}. \tag{7}$$

The image currents associated with the P_i patches are

$$\vec{J}'(\vec{r}') = \left(-J_x\hat{x} - J_y\hat{y} + J_z\hat{z}\right)e^{-j\vec{K}^n\cdot\vec{r_s'}}, \tag{8}$$

where

$$\vec{K}^n = K_x^i\hat{x} + K_y^i\hat{y} - K_z^i\hat{z}. \tag{9}$$

The contribution to the far field in the backscattering direction is obtained by using the PO integral of the image currents. The finite dimension of the patches is taken into account via ray tracing [29], so only the illuminated region of the facets (see Figure 11) is considered.
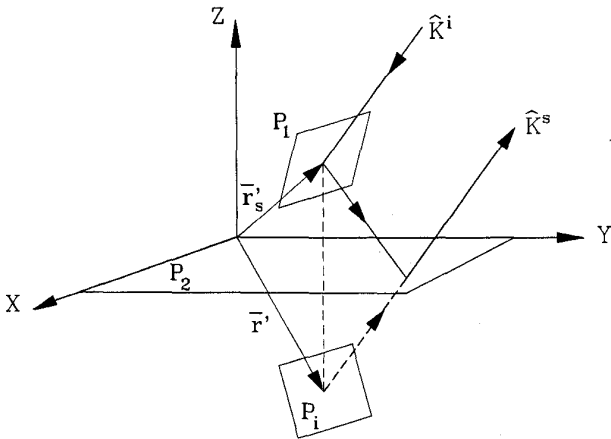

Figure 10. A dihedral is formed by facets P_1 and P_2. Facet P_i is the image of P_1 over the plane that contains facet P_2.
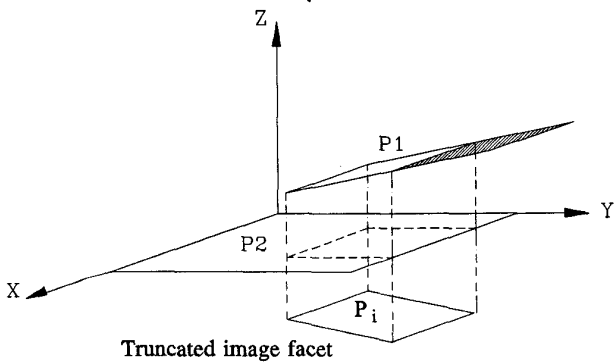

Truncated image facet

Figure 11. The dashed part of P_1 is excluded when the image facet P_i is defined.
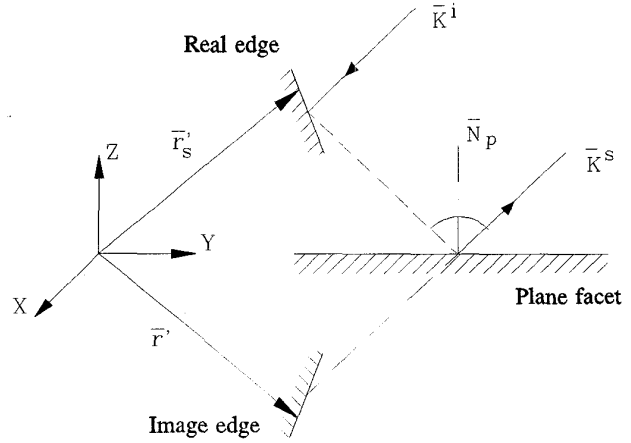

Figure 12. In the analysis of the diffraction-reflection process between an edge and a plane facet, an equivalent-image edge is substituted for the edge.
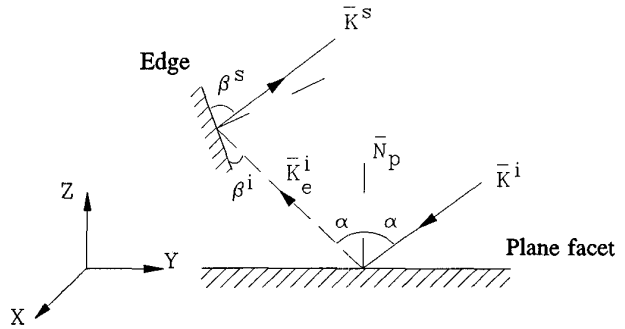

Figure 13. In the reflection-diffraction process, a reflected plane wave is assumed incident over the edge.

6.2 Diffracted-reflected field

This mechanism is an improvement for the double reflections between patches. This contribution to the backscattered field can be calculated by considering two terms: a field diffracted from the edge and then reflected in the conductor plane (DR), and a term due to the field first reflected and then diffracted from the edge (RD). These terms are calculated by using the ECM approach, in combination with image theory [3].

In the case of the DR (see Figure 12) process, we use image theory, which is equivalent to the classical GO assumption. In the RD (see Figure 13) process, we consider the plane-wave nature of the field that is incident on the facet to not be changed after reflection. The *TOTAL* backscattered field created is obtained by adding the diffraction-reflection contribution to the reflection-diffraction contribution

$$\vec{E}_{TOTAL} = \vec{E}_{DR} + \vec{E}_{RD}. \tag{10}$$

Errors can appear if the size of the facets is not taken into account when the image currents are computed. This problem is solved, via ray tracing, by analyzing the intersection of the diffracted ray with the flat facet. To take into account the actual size of the facets, the edges are subdivided into several segments. Each segment is represented by its center point (see Figure 14). In this
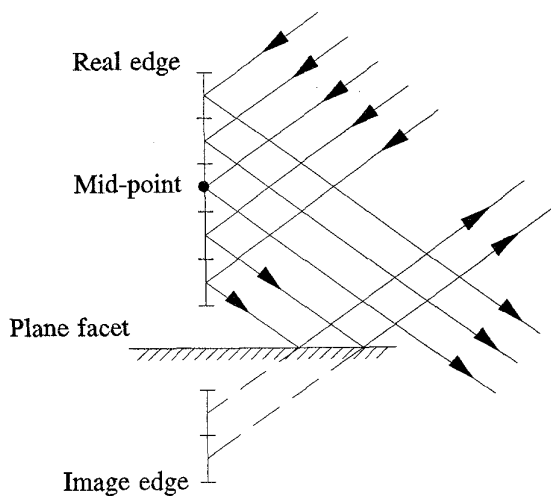
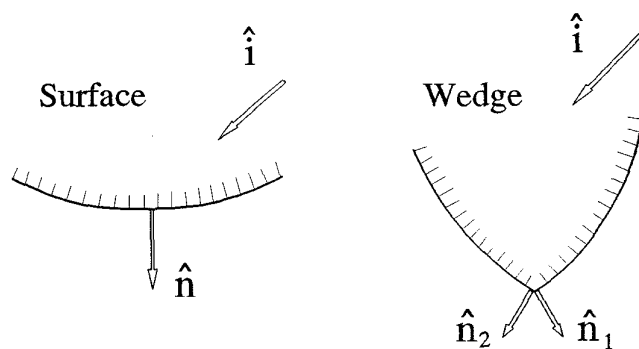Figure 14. An example of the subdivision of edges.

Figure 15. Examples of hiding by self shadowing.

example, it can be observed that there are only a few segments on the edges that must be taken into account. Only the field radiated from the image of these segments is considered.

7. Shadowing

If a surface, a wedge, or a part of these is not illuminated by the incident wave, the contribution to the reflected or diffracted field must be ignored. There are two possibilities for surfaces becoming hidden:

• Self-shadowing or outward-normal shadowing
• Eclipse-shadowing, sometimes referred to as cast or mutual shadowing

The first case appears when a surface is illuminated from its back face. That is, the scalar product between the unit normals ($\hat{n}$) and the incident direction ($\hat{i}$) is negative (see Figure 15). In the case of an edge, the self-shadowing analysis involves two scalar products related to the normal vectors of the two surfaces ($\hat{n}_1$ and $\hat{n}_2$) which form the wedge, as can be seen in Figure 15.

In curved patches, the unit-normal vector varies along the surface, so a part of the surface can be illuminated and the other part, hidden. But, as mentioned before, the scattering centers on curved surfaces are critical points or segments. Therefore, the self-

shadowing analysis is simplified considerably, taking only the critical points into account.

The eclipse-shadowing analysis is a more-complicated task. This is produced when a scattering center is hidden by another part of the body. Given a scattering center, the problem lies in determining whether is hidden by any illuminated NURBS surface of the body.

A generic plane surface can be completely hidden, partially hidden, or illuminated. In the first case, its contribution is removed, and in the second, the surface is clipped, and only the contribution of the illuminated part is considered. For this purpose, a set of points (named sample points) is selected on a given illuminated NURBS patch (see Figure 16). For each incident direction, these points are projected onto the plane which contains the facet being studied. The result of this process is a set of points located on the plane. The convex-hull polygon enclosing them is achieved, in order to obtain the resulting shadow region. When this task has been performed, it is easy to study the shadowing of the plane surface by the NURBS patch. If all the vertex points of the facet are located inside the convex-hull polygon, the facet is completely shadowed. If the facet has vertex points inside and outside the convex-hull polygon, it is partially shadowed, and it is clipped by using the Weley-Altherton algorithm [29].
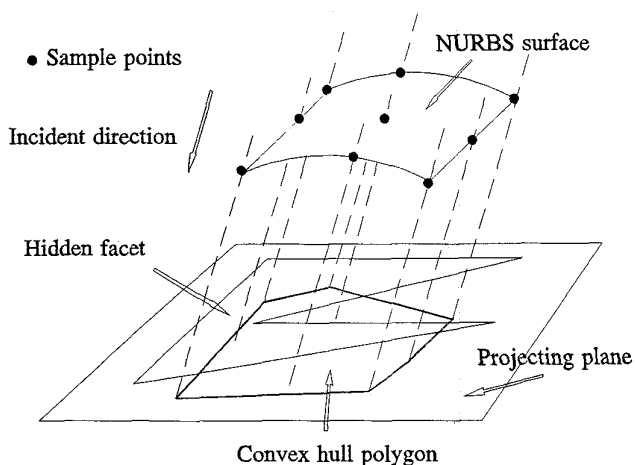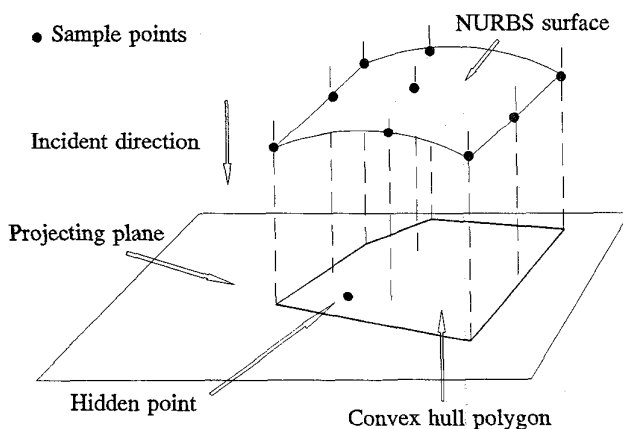

Figure 16. Plane-facet hiding.
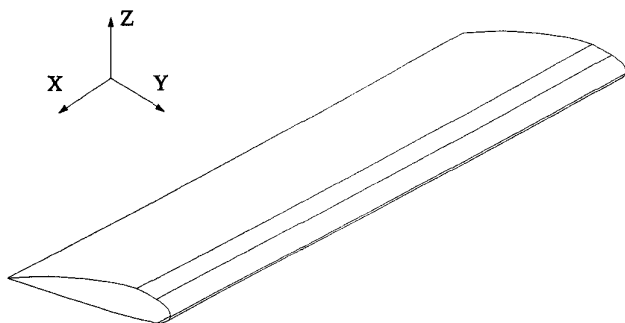

Figure 17. Point hiding.

Figure 18. A NURBS-patch model of the NACA 3317 airfoil (30" × 6").
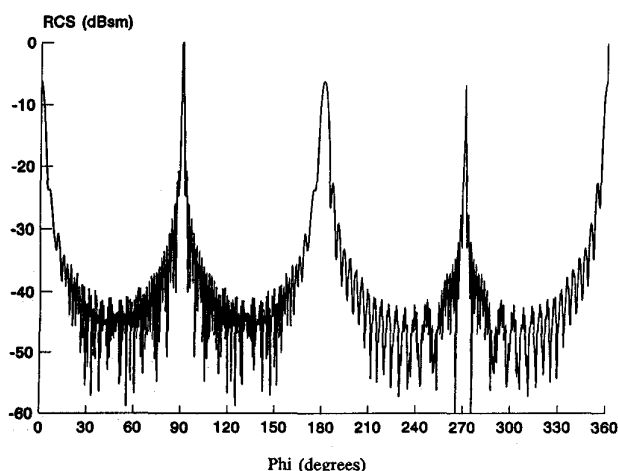

Figure 19. The RCS for the NACA 3317 airfoil computed with the *TOTAL* code (horizontal polarization at 16 GHz).

The study of the eclipse-shadowing of wedges, critical points, and segments, is easier than in flat surfaces. In the present approach, the critical segments and wedges are considered to be hidden if their mid-points are shadowed. Therefore, the eclipse-shadowing problem in curved surfaces and wedges is reduced to analyzing if a point is hidden or not. To check if a given point is hidden, all the illuminated NURBS surfaces, located ahead of the point, are taken into account. For each incident wave, the sample points of each NURBS surface are projected onto a plane perpendicular to the incident direction (see Figure 17), and a test is performed to determinate if the points are inside or outside the corresponding convex-hull polygon.

8. Results

Numerical results of the *RANURS* code for complex geometries are presented below. Results about low- and medium-complexity targets can be seen in references [3, 7, 8].

7.1 NACA 3317 airfoil

This geometry has been analyzed with the *TOTAL* and *RANURS* codes. The model for *RANURS* contains six surfaces and one edge (see Figure 18), whereas in *TOTAL*, the model is described by 53 flat patches and 89 straight edges. Figures 19 and

20 show the RCS results obtained with *TOTAL* and *RANURS* for the $\theta = 90°$ cut. These results are very close to the measured values that appear in reference [1], which have been reproduced in Figure 21.

7.2 Generic missile

Figures 2a and 2b present two models of the missile which was analyzed. The first one is an edge-facet model of the missile that is described by 639 flat patches and 1,122 straight edges. The second figure represents a NURBS-surfaces model which contains 57 patches. Figures 22 and 23 show predicted RCS values for the $\theta = 90°$ cut and vertical polarization at 12 GHz. These results have been obtained by taking into account reflections, diffractions, and double interactions. Comparing these numerical results with the measurements in [1], a good agreement can be observed.

7.3 CN235 airplane

This target was modeled by 15,886 flat facets and 26,037 edges for the *TOTAL* code, and with 104 NURBS surfaces and 72 edges for the *RANURS* code. A sketch of the NURBS-patches model is shown in Figure 1. Figure 24 presents measurements
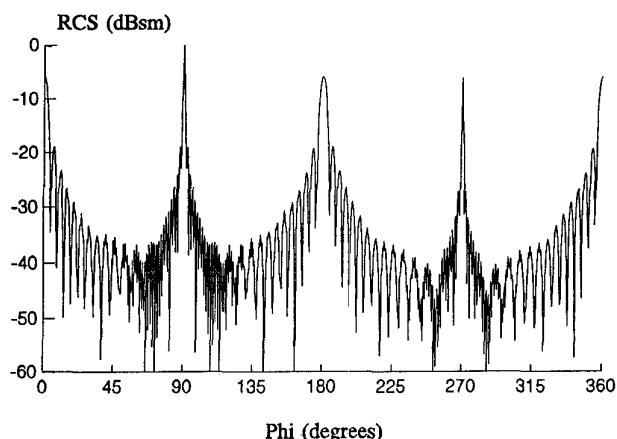

Figure 20. The RCS for the NACA 3317 airfoil computed with the *RANURS* code (horizontal polarization at 16 GHz).
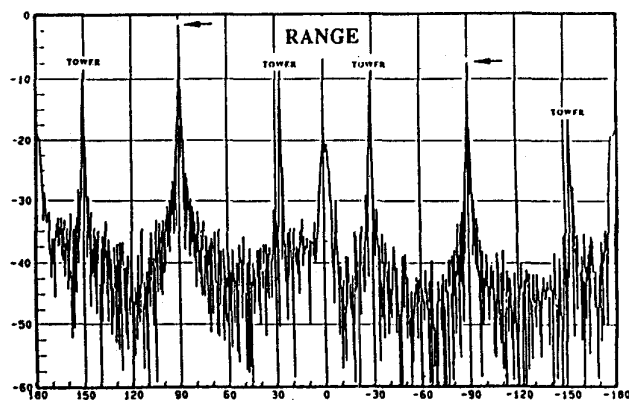

Figure 21. The measured RCS for the NACA 3317 airfoil (horizontal polarization at 16 GHz), taken from [1].
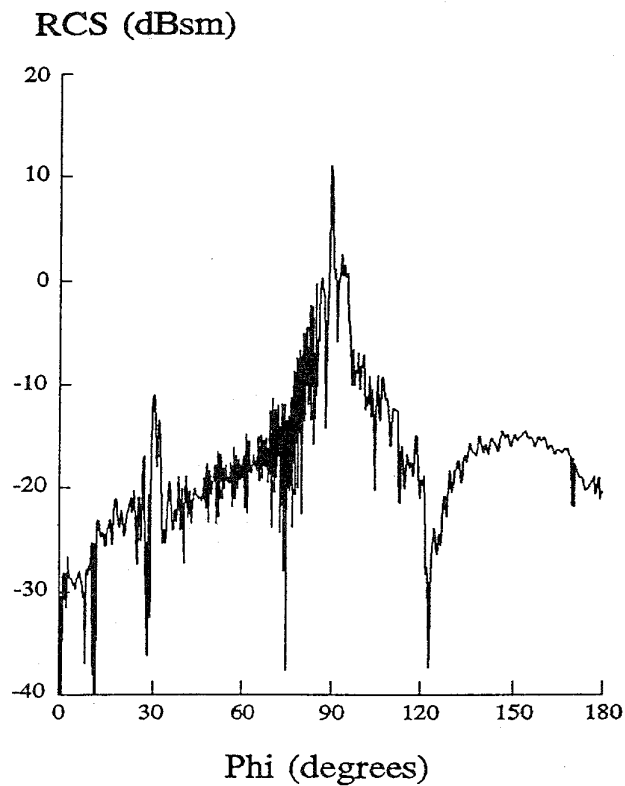
RCS (dBsm)

Figure 22. The RCS for the generic missile computed with the *TOTAL* code (vertical polarization at 12 GHz).
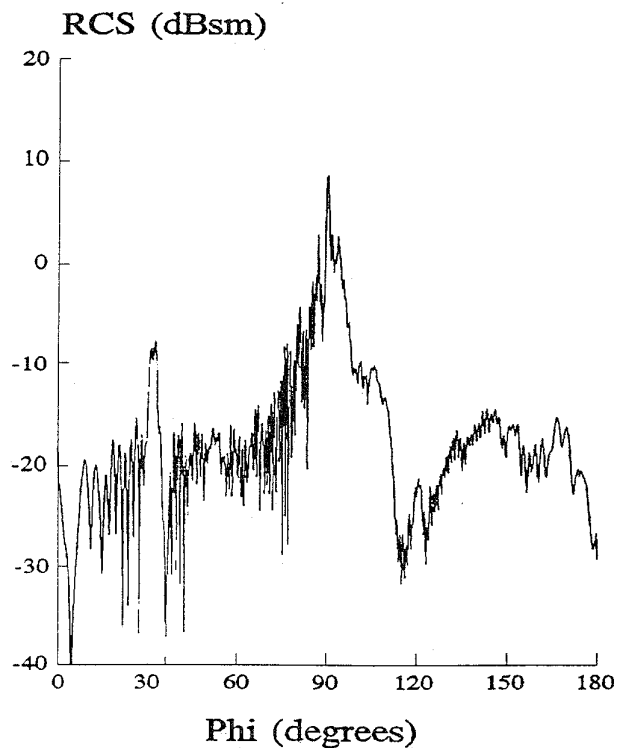
RCS (dBsm)

Figure 23. The analytical RCS for the generic missile computed with the *RANURS* code (vertical polarization at 12 GHz).
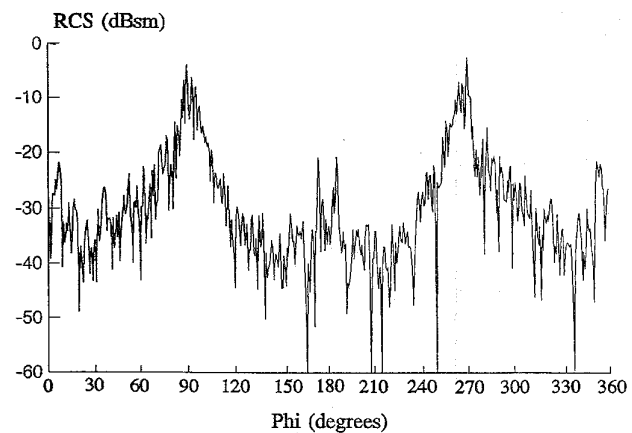
RCS (dBsm)

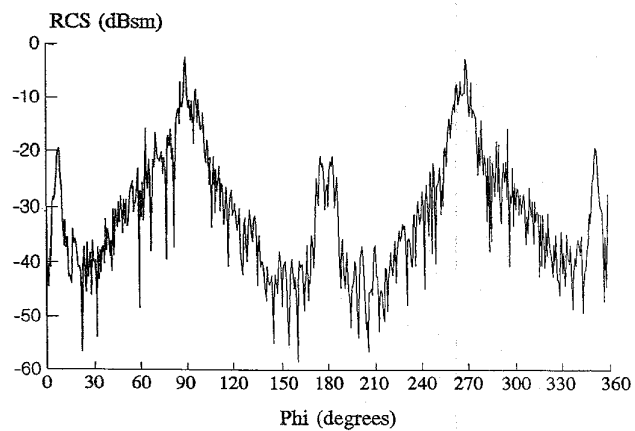Figure 24. The measured RCS for the CN235 airplane.

RCS (dBsm)

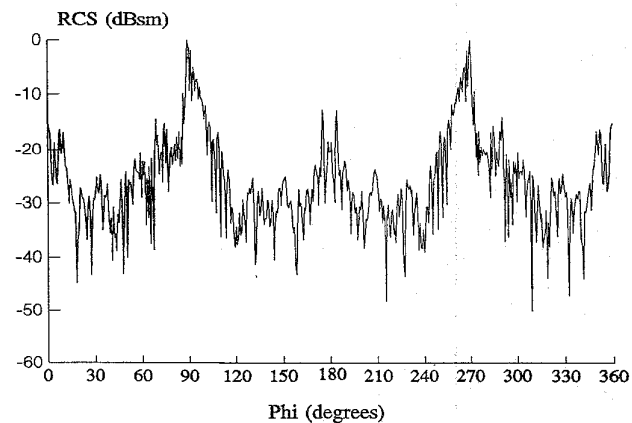Figure 25. The RCS for the CN235 airplane computed with the *RANURS* code.

RCS (dBsm)

Figure 26. The RCS for the CN235 airplane computed with the *TOTAL* code.

Table 1. CPU times for the *TOTAL* code.

Target Modeled	No. Patches	No. Edges	RCS Contributions	CPU Time
NACA 3317 Airfoil	53	89	Reflections and diffractions	0:00:06
Missile	639	1122	Reflections and diffractions	0:01:01
			Reflections, diffractions, and double interactions	0:22:36
CN235 Airplane	15886	26037	Reflections and diffractions	0:19:32

Table 2. CPU times for the *RANURS* code.

Target Modeled	No. Patches	No. Edges	RCS Contributions	CPU Time
NACA 3317 Airfoil	7	15	Reflections and diffractions	0:00:18
Missile	57	79	Reflections and diffractions	0:31:30
			Reflections, diffractions and double interactions	0:32:10
CN235 Airplane	86	72	Reflections and diffractions	0:16:46
			Reflections, diffractions and double interactions	2:54:50

obtained from a 1/76 scale model for the $\theta = 90°$ cut at 26 GHz. These measurements were carried out by the Department of Signal Theory and Communications of the Universitat Politécnica de Catalunya, in Barcelona, Spain. Figure 25 shows the RCS values obtained with *RANURS*. As can be observed, the shape of the curve, and the positions of maxima and minima, agree well with the measured values. Figure 26 shows the RCS values obtained with *TOTAL*. In both cases, the results have been obtained by considering single and double effects.

7.4 CPU times

Tables 1 and 2 show the CPU times obtained by the *TOTAL* and *RANURS* codes for different geometries. The computer was a HP Apollo 735 (124 MIPS; 41 MFLOPS). If only reflected and diffracted contributions to the RCS are considered, it can be observed in Tables 1 and 2 that the CPU times vary from several seconds, for simple geometries, to nearly half an hour, for complex, realistic targets. When considering double interactions, the run times grow very much. This fact must be taken into account by the users, who should chose this option only for the angular margins, where non-negligible RCS due to double interactions can be anticipated.

The memory-size requirements are basically dependent on the complexity of the models. For instance, in the worst case (the CN235 airplane), the RAM-memory requirements for *TOTAL* and *RANURS* are 10 megabytes and 4 megabytes, respectively. There-fore, these codes are suitable for running on a compatible PC of high performance, with reasonable CPU times.

9. Conclusions

This paper has presented a general-purpose code, *RANURS*, for use in the analysis of the monostatic RCS of electrically large, complex targets. The geometrical description of the targets is given in terms of NURBS surfaces. This technique of modeling is used in a variety of industries (aircraft, ships, cars, etc.), and by engineers involved in different aspects of the design process (structural, mechanical, aerodynamical, electrical, etc.). The NURBS surfaces can be generated by the most-common CAGD tools, so *RANURS* can be easily integrated with many of the available CAGD codes. In fact, it has been integrated with the *I-DEAS* solid-modeling tool.

The classical RCS analysis packages usually describe the targets in terms of facets and wedges. However, the NURBS-surfaces technique requires less memory storage to describe the targets' geometries, enabling more accurate adjustment to the real target surface. This avoids the "facet noise" usually present in classical facet-modeling codes.

The scattered fields are calculated by using the PO+EMC approach. These high-frequency techniques are very efficient and accurate, when used in combination with a NURBS description of the scatterers. First, this is true because a small number of patches are used to model the target accurately. Second, it is also due to the fact that the PO+EMC approach is directly applied on the parametric surfaces, and the final expressions of the fields are given as functions of the NURBS-patch coefficients.

The contributions to the RCS can be subdivided into single effects (reflected fields and diffracted fields) that can be computed in very little time, and double effects (double-reflected fields, reflected-diffracted fields, and diffracted-reflected fields), which need more computational resources. In addition the shadowing problem has been efficiently addressed.

The program has been thoroughly validated. The paper shows some results of comparisons with measurements and numerical simulations from other codes. Data about computer times have also been presented. Finally, it is possible, with some additional effort, to modify *RANURS* for the treatment of different materials (finite conductivity, RAM, etc.).

To obtain further information about both codes, contact Felipe Cátedra at +34-42-201873 (Fax), or send e-mail to felipe@gsr.unican.es.

10. Acknowledgments

11. References

1. N. N. Youssef, "Radar Cross Section of Complex Targets," *Proceedings of the IEEE*, 77, 5, May 1989, pp. 722-734.

2. Marta Domingo, *Application of high frequency techniques to the RCS prediction of complex bodies modelled with plane facets* (in Spanish), Tesis Doctoral, Universidad de Cantabria, España, Julio 1994.

3. M. Domingo, R. P. Torres, M. F. Cátedra, "Calculation of the RCS from the interaction of edges and facets," *IEEE Transactions on Antennas and Propagation*, **AP-42**, June 1994, pp. 885-888.

4. G. Farin, *Curves and Surfaces for Computer Aided Geometric Design*, Academic Press, 1988.

5. W. Boehm, G. Farin, J. Kahmann, "A Survey of Curve and Surface Methods in CAGD," *Computer Aided Geometric Design*, **1**, 1984, pp. 1-60.

6. W. Tiller, "Rational B-Splines for Curve and Surface Representation," *IEEE Computer Graphics and Applications*, **3**, September 1983, pp. 61-69.

7. J. Pérez, M. F. Cátedra, "RCS of Electrically Large Targets Modelled with NURBS Surfaces," *Electronic Letters*, **28**, 12, June 1992, pp. 1119-1121.

8. J. Pérez, M. F. Cátedra, "Application of the Physical Optic to the RCS computation of bodies modelled with NURBS surfaces," *IEEE Transactions on Antennas and Propagation*, **AP-42**, 10, October 1994, pp. 1404-1411.

9. J. Pérez, *Application of the Physical Optic to the RCS computation of complex bodies modelled with NURBS patches* (in Spanish), doctoral thesis, University of Cantabria, Spain, 1994.

10. J. M. Rius, M. Ferrando, L. Jofre, "GRECO: Graphical Electromagnetic Computing for RCS Prediction in Real Time," *IEEE Antennas and Propagation Magazine*, **35**, 2, April 1993, pp. 7-17.

11. A. García-Pino, F. Obelleiro, J. L. Rodríguez, A. M. Arias, "A comparison of ray tracing methods for the analysis of high frequency scattering by arbitrary shaped cavities," *IEEE Antennas and Propagation International Symposium and USNC/URSI National Radio Science Meeting Digest of URSI Abstracts*, Chicago, Illinois, July 1992, pp. 505.

12. L. Valle, F. Rivas, M. F. Cátedra, "Combining the Moment Method with geometrical modeling by NURBS surfaces and Bezier patches," *IEEE Transactions on Antennas and Propagation*, **AP-43**, 3, March 1994, pp. 373-381.

13. J. Sainz, J. Pérez, O. Conde, R. Torres, M. F. Cátedra, "GONURBS: A numerical code to analyze antennas on board of complex structures modelled with NURBS surfaces," *Abstracts of PIERS'94*, Noordwijk, The Netherlands, July 1994, pp. 328.

14. D. M. Elking, J. M. Roedder, D. D. Car, S. D. Alspach, "A Review of High-Frequency Radar Cross Section Analysis Capabilities at McDonnell Douglas Aerospace," *IEEE Antennas and Propagation Magazine*, **37**, 5, October 1995.

15. IGES, "Initial Graphics Exchange Specifications, Version 3.0," Doc. No. NB-SIR 86-3359, National Bureau of Standards, Gaithersburg, MD, USA, 1986.

16. *I-DEAS Geomod Users Guide*, Structural Dynamics Research Corporation (SDRC), Milford, OH 45150, USA.

17. W. Boehm, "Generating the Bezier points of B-Spline Curves and Surfaces," *Computer Aided Design*, **13**, 16, 1981, pp. 365-366.

18. E. F. Knott, "A Progression of High-Frequency RCS Prediction Techniques," *Proceedings of the IEEE*, **73**, 2, February 1985, pp. 252-264.

19. G. T. Ruck, D. E. Barrick, W. D. Stuart, C. K. Krichbaum. *Radar Cross Section Handbook*, New York, Plenum Press, 1970, Chapter 2.

20. R. G. Kouyoumjian, "Asymptotic High-Frequency Methods," *Proceedings of the IEEE*, **53**, August 1965, pp. 864-876.

21. W. B. Gordon, "Far-Field Approximation to the Kirchhoff-Helmholtz Representations of Scattered Field," *IEEE Transactions on Antennas and Propagation*, **AP-23**, July 1975, pp. 864-876.

22. D. S. Jones, M. Kline, "Asymptotic expansions of multiple integrals and the method of the stationary phase," *Journal of Mathematical Physics*, 37, January 1957, pp. 1-28.

23. E. F. Knott, J. F. Shaeffer, M. T. Tuley, *Radar Cross Sections*, Norwood, MA, Artech House, Inc., 1985, Chapter 5.

24. P. Ya. Ufimtsev, "Elementary Edge Waves and the Physical Theory of Diffraction," *Electromagnetics*, **11**, 2, April-June 1991, pp. 125-160.

25. T. Griesser, C. A. Balanis, "Backscatter Analysis of Dihedral Corner Reflectors Using Physical Theory of Diffraction," *IEEE Transactions on Antennas and Propagation*, **AP-35**, 10, October 1987, pp. 1137-1147.

26. T. Griesser, C. A. Balanis, "Dihedral Corner Reflectors Backscatter Using High Order Reflections and Diffractions," *IEEE Transactions on Antennas and Propagation*, **AP-35**, 11, November, 1987, pp. 1235-1247.

27. E. F. Knott, "RCS Reduction of Dihedral Corners," *IEEE Transactions on Antennas and Propagation*, **AP-25**, 3, May 1977, pp. 406-409.

28. R. G. Atkins, R. T. Shin, "A Physical Optics Technique for prediction of multiple reflections from polygonal plate structures," *Journal of Electromagnetic Waves and Applications*, **2**, 8, 1988, pp. 687-712.

29. D. F. Rogers, *Procedural Elements for Computer Graphics*, Singapore, McGraw-Hill International Editions, Computer Science Series, 1985.

Introducing Feature Article Authors

Marta Domingo was born in Santander, Spain, in 1962. She received the MS degree in Physics from the University of Cantabria, Spain, in 1989, and the PhD in Physics from the University of Cantabria, in 1994. From 1989 to 1990, she was with the Radio Communication and Signal Processing Department of the UPM as a research assistant. During this time, she worked on high-frequency methods applied to RCS computation.

In 1990, she joined the Electronics Department of the University of Cantabria as a research assistant, where she has been working on several projects dealing with RCS computation, analysis of antennas on board structures, and electromagnetic compatibility. In 1993, she become an Assistant Professor in the Electronics Department of the University of Cantabria. Her current research interests include high-frequency methods in electromagnetics and numerical methods.

Fernando Rivas was born in Santander, Spain, in 1966. He received the MS degree in Physics from the University of Cantabria, Spain, in 1989, and the PhD in Physics from the University of Cantabria, in 1994.

He has been with the Electronics Department, University of Cantabria since 1989. His research interests are in the areas of numerical analysis of electromagnetic radiation, scattering problems, and geometrical modeling in electromagnetics.

Jesús Pérez was born in Santander, Spain, in 1965. He received the MS degree in Physics from the University of Cantabria, Spain, in 1989, and the PhD in Physics from the University of Cantabria, in 1994. From 1989 to 1992, he was with the Electronics Department of the University of Cantabria as a research assistant.

In 1993, he become an Assistant Professor in the Electronics Department of the University of Cantabria. His areas of interest include electromagnetic radiation and scattering, geometrical modeling in electromagnetics, and mobile communications.

Rafael Torres was born in Málaga, Spain, in 1961. He received his MS degree in Physics from the University of Granada, Spain, in 1986, and his PhD in Telecommunications Engineering from the Polytechnic University of Madrid (UPM), in 1990. From 1986 to 1990, he was with the Radio Communication and Signal Processing Department of the UPM as a research assistant. During this time, he worked on numerical methods in electromagnetics, and their applications to the design of passive-microwave devices such as radomes, circular polarizers, rotators, and planar lenses.

He became an Associate Professor in the Electronics Department of the University of Cantabria, Spain, in 1990. From that time to the present, he has participated in several projects on RCS computation, onboard-antenna analysis, and electromagnetic compatibility. He is co-author of a book about the CG-FFT method, several chapters in different books, papers, and about 30 conference contributions. His research interests include numerical and high-frequency methods in electromagnetics applied to antennas, radio-propagation, and mobile communications, and microwave components.

Manuel F. Cátedra received his MS and PhD degrees in Telecommunications Engineering from the Polytechnic University of Madrid (UPM), in 1977 and 1982, respectively. From 1976 to 1989, he was with the Radiocommunication and Signal Processing Department of the UPM, teaching and doing research. He became a full Professor at Cantabria University in 1989.

He has worked on about 25 research projects, solving problems of electromagnetic compatibility in radio and telecommunication equipment, antennas, microwave components, and radar cross section and mobile communications. He has developed and applied CAD tools for radio-equipment systems such as warships, aircraft, helicopters, and satellites. The main contractors for this work have been Spanish or European institutions such as CASA, ALCATEL, BAZAN, the Spanish Defence Department, and the French company, MATRA. He has directed about ten PhD dissertations, has published about 20 papers, a book, about 10 chapters in other books, and has presented around a hundred communications at international symposia. ⊛
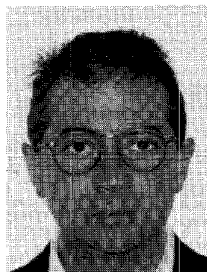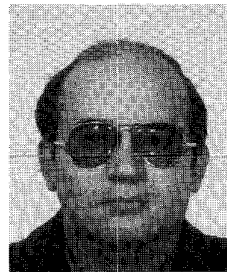
Marta Domingo
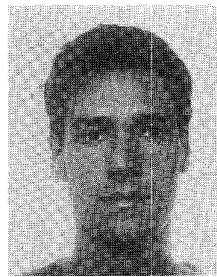
Fernando Rivas

Jesús Pérez

Rafael Torres

Manuel F. Cátedra